Supporting Information

Highly efficient and stable low-temperature processed ZnO solar cells with triple cation perovskite absorber

Jiaxing Song,[a] Leijing Liu,[a] Xiao-Feng Wang,[b,*] Gang Chen,[b] Wenjing Tian,[a,b,*] and Tsutomu Miyasaka[c]

[a] State Key Laboratory of Supramolecular Structure and Materials, Jilin University, Changchun 130012, PR China

[b] Key Laboratory of Physics and Technology for Advanced Batteries, Ministry of Education, College of Physics, Jilin University, Changchun 130012, PR China

[c] Graduate School of Engineering, Toin University of Yokohama, 1614 Kurogane-cho, Aoba, Yokohama, Kanagawa225-8503, Japan

*E-mails: xf_wang@jlu.edu.cn(X.-F. Wang) and wjtian@jlu.edu.cn (W. Tian)

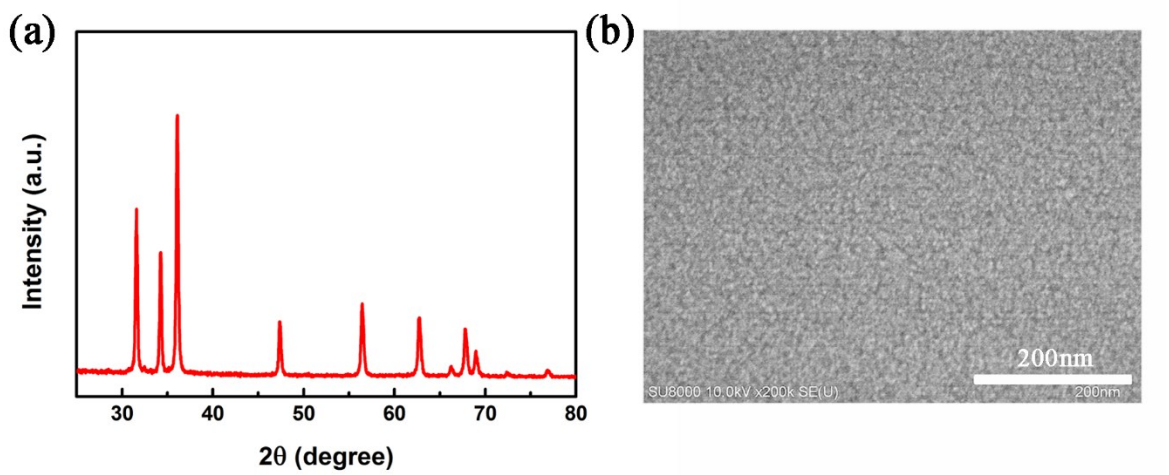

Figure S1. (a) The XRD pattern of the ZnO nanoparticles and (b) the high magnification SEM micrograph of ITO/ZnO film.

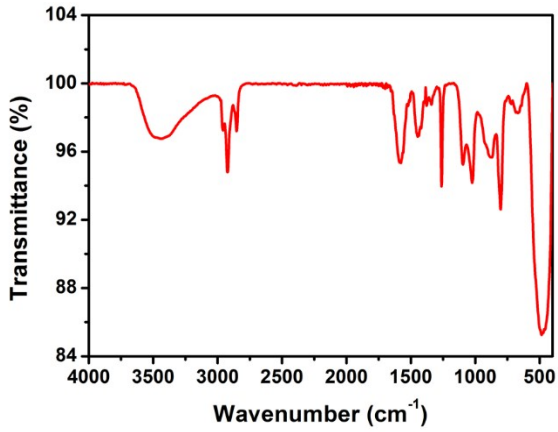

Figure S2. The FT-IR spectrum of ZnO film processed at low temperature.

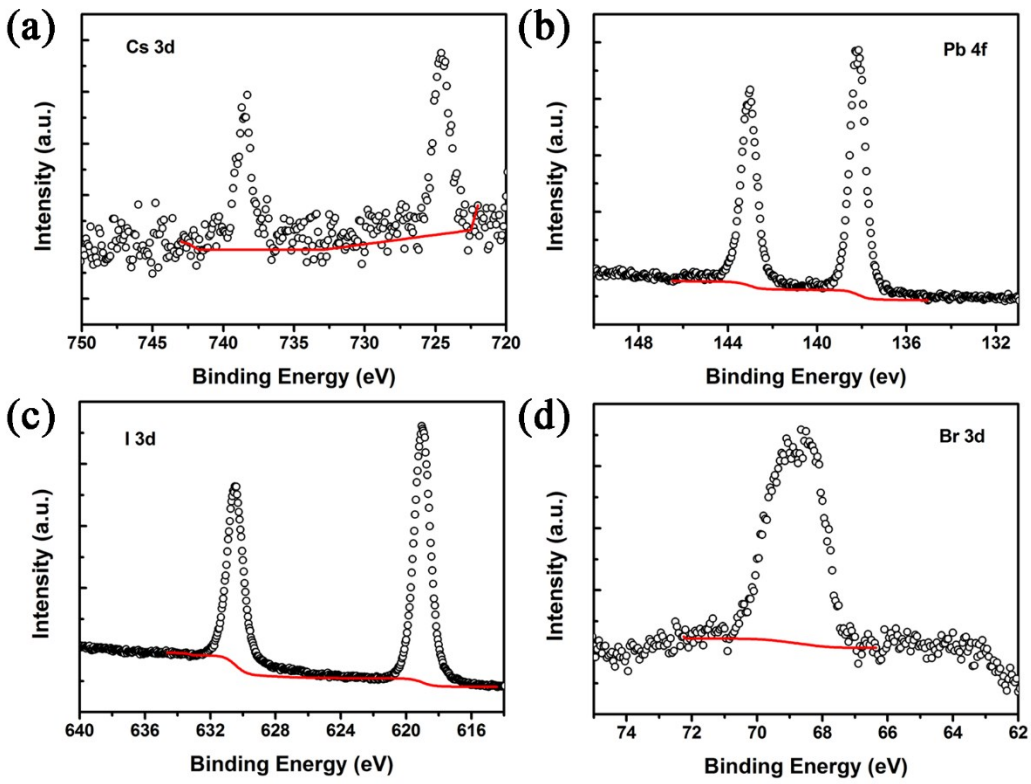

Figure S3. The chemical composition of Cs_6M from XPS results. (a) Cs 3d, (b) Pb 4f, (c) I 3d and (d) Br 3d core level spectra.

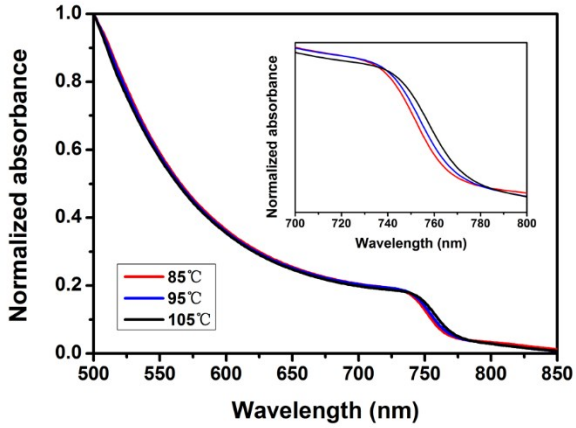

Figure S4. UV-vis-NIR absorption spectra of $Cs_{10}M$ films obtained from the perovskite layers with different annealing temperature. The inset is the enlarged view of the absorption spectra at absorption edge.

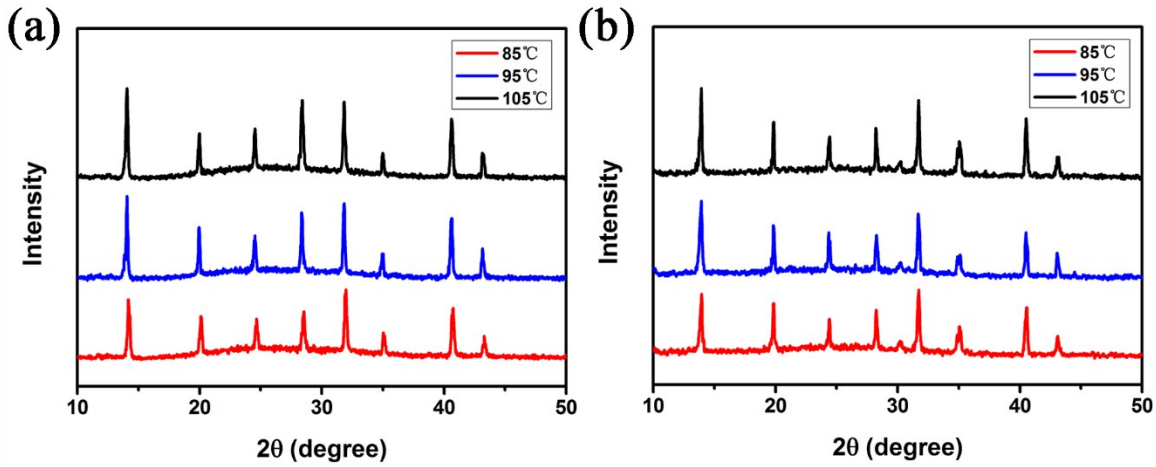

Figure S5. X-ray diffraction patterns of (a) ITO/TiO_2/$Cs_{10}M$ and (b) ITO/$Cs_{10}M$ thin films obtained from the different annealing temperature.

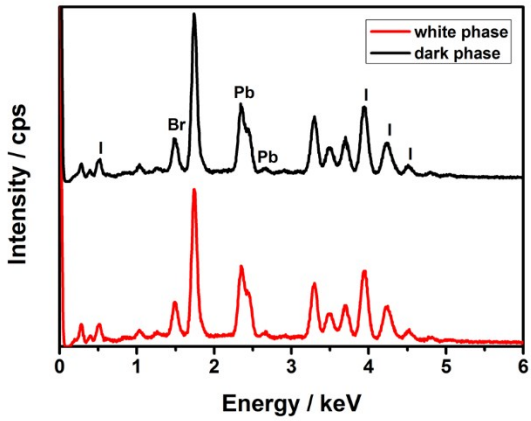

Figure S6. The EDX patterns for the perovskite layer in the white phase and dark phase, respectively.

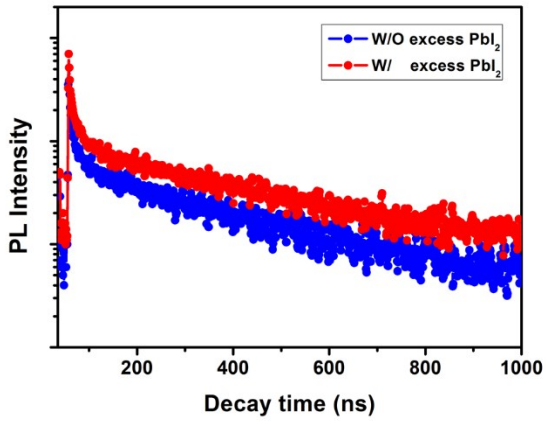

Figure S7. Time resolved photoluminescence (TrPL) spectra of Cs_6M films with and without remnant PbI_2 phase. The later was annealed at 85 °C for 4 min.

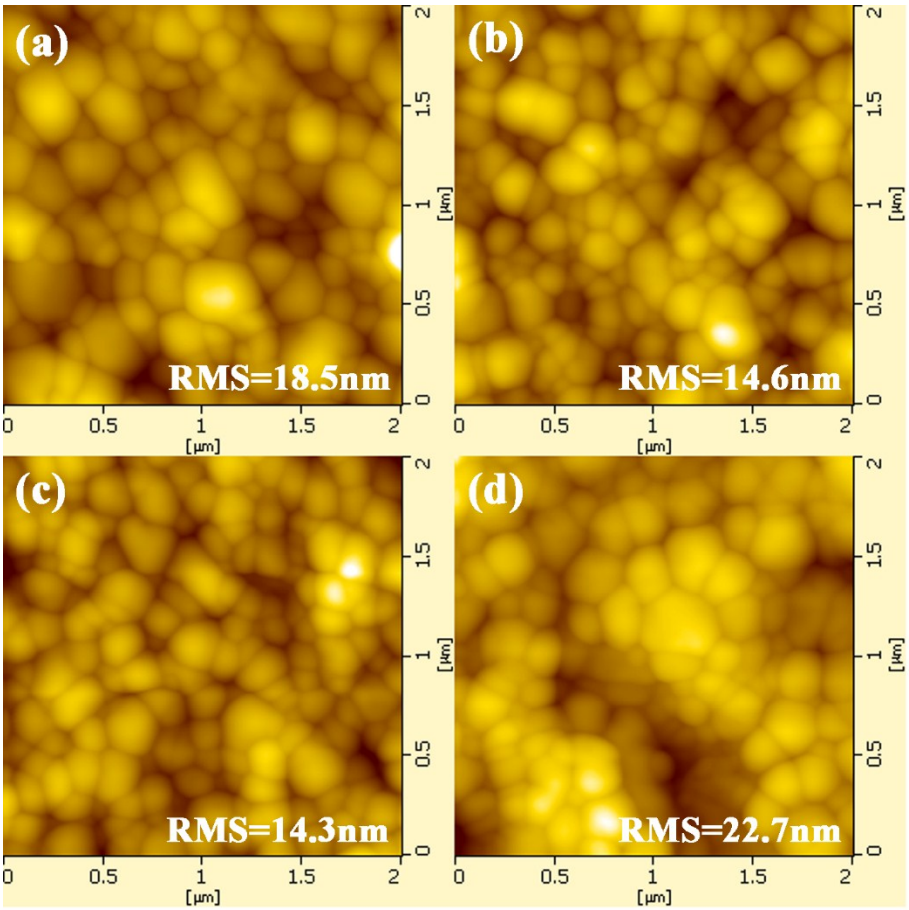

Figure S8. AFM images of the Cs_xM series with (a) Cs_2M, (b) Cs_6M, (c) $Cs_{10}M$ and (d) $Cs_{14}M$, and corresponding RMS roughness are also presented therein.

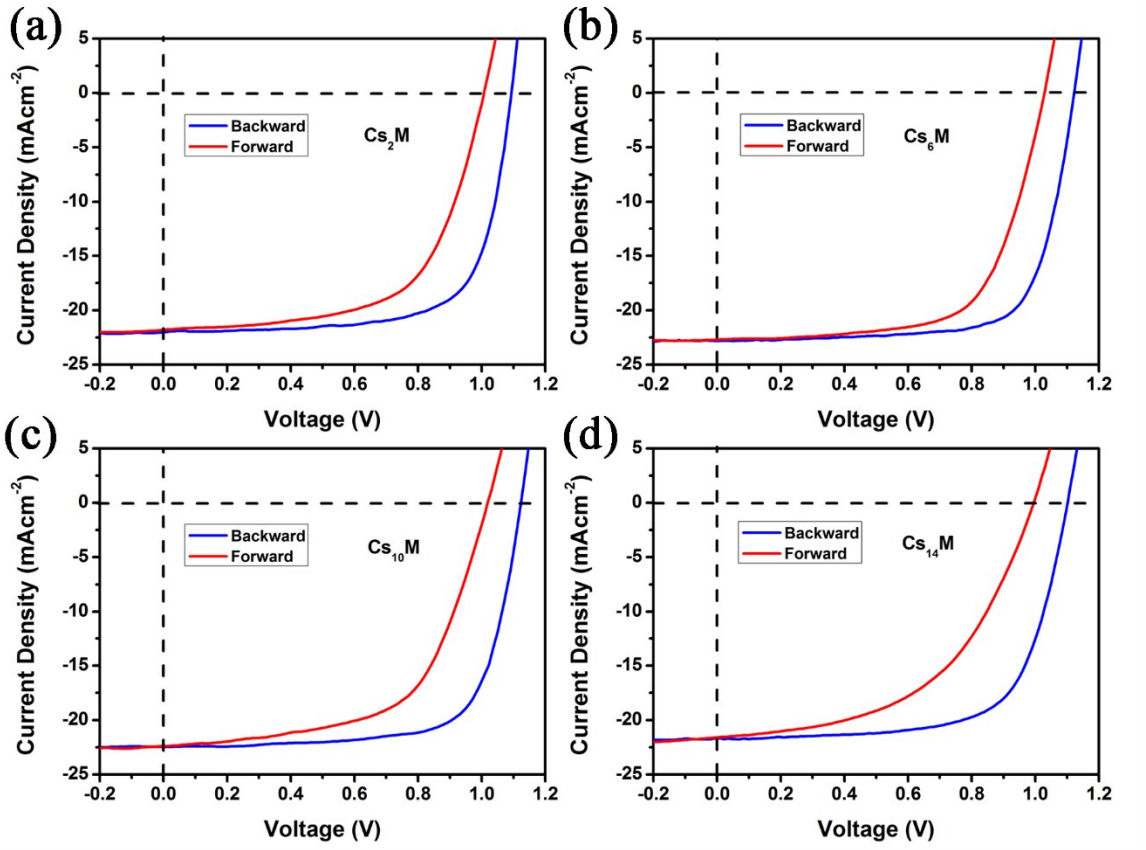

Figure S9. The *J-V* characteristics of the devices based on the Cs_xM series measured at 100 $mWcm^{-2}$ AM 1.5G illumination under different scanning directions.

Table S1. The corresponding photovoltaic performance parameters for PSCs under different scanning directions in Figure S4.

		V_{oc} / V	J_{sc} / $mAcm^{-2}$	FF / %	PCE / %
Cs_2M	forward	1.01	21.8	61.9	13.6
	backward	1.09	22.0	71.1	17.1

Cs_6M	forward	1.03	22.7	65.9	15.4
	backward	1.12	22.8	72.8	18.6
$Cs_{10}M$	forward	1.02	22.4	59.9	13.7
	backward	1.12	22.5	72.0	18.1
$Cs_{14}M$	forward	1.0	21.6	50.9	11.0
	backward	1.10	21.7	68.2	16.3

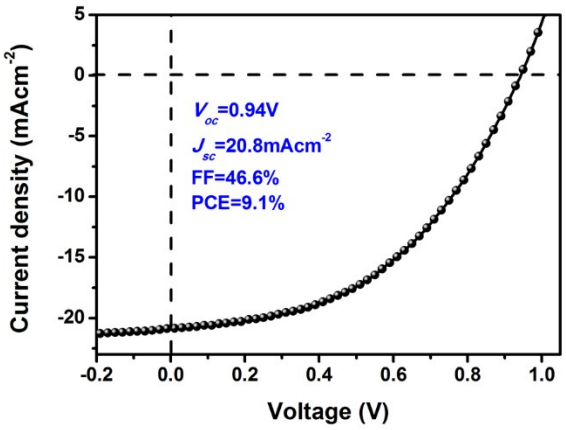

Figure S10. *J-V* characteristic of the best-performing ITO/ZnO/$MAPbI_3$/spiro-OMeTAD/Ag device.

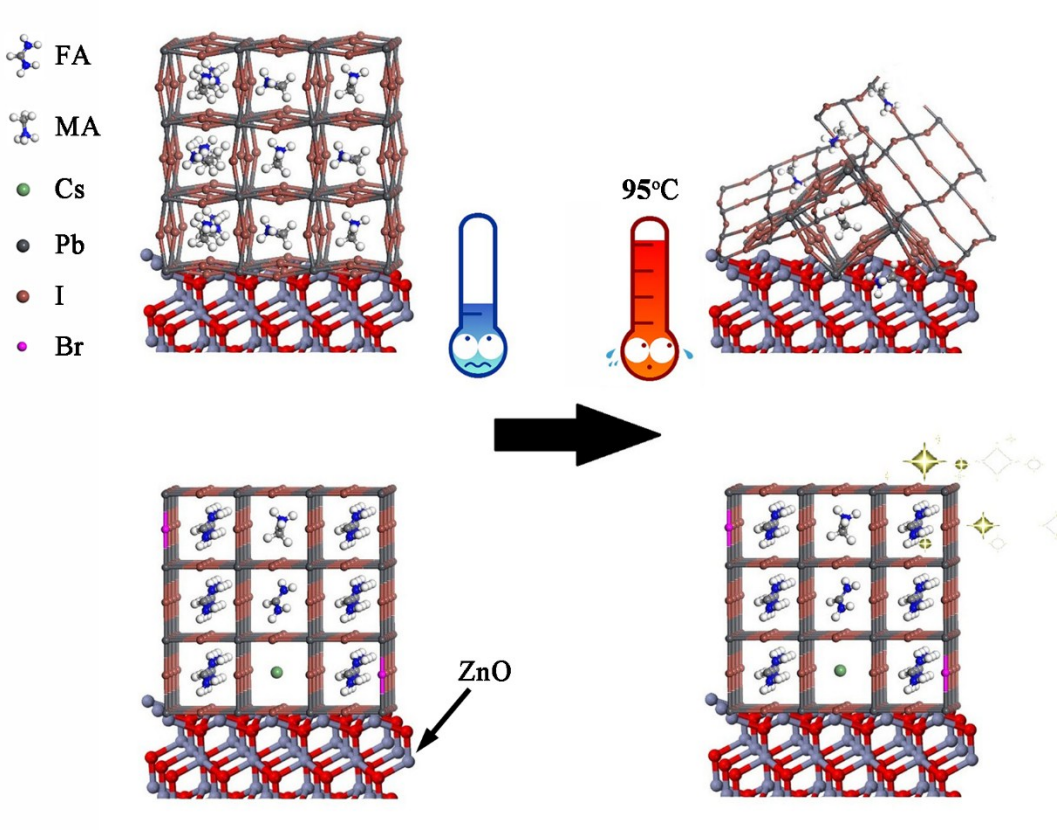

Figure S11. A structurally graphical image displaying the variation when using the triple-cation recipe as an alternative to $MAPbI_3$ on low-temperature processed ZnO.

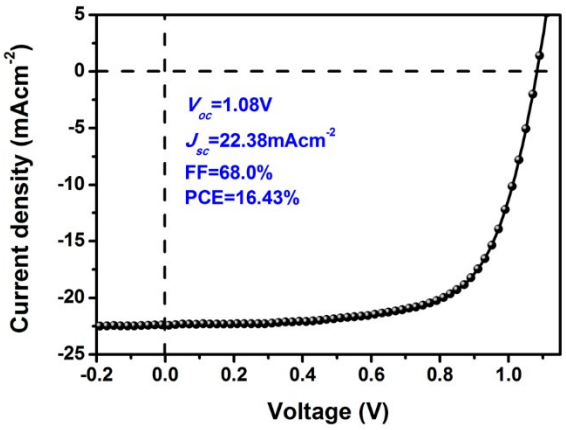

Figure S12. *J-V* characteristic of the best-performing ITO/TiO_2/Cs_6M/spiro-OMeTAD/Ag device.

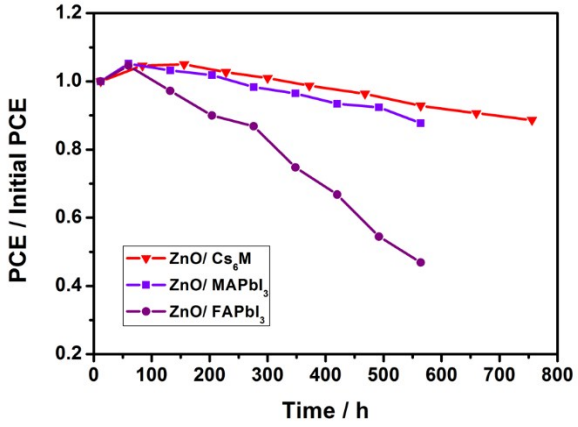

Figure S13. Durability of the ZnO-based Cs_6M, $MAPbI_3$ and $FAPbI_3$ PSC devices stored in the ambient condition.